Supporting Information

Selectively Photocatalytic Activity of an Open Framework Chalcogenide Built from Corner-sharing T4 Supertetrahedral Clusters

Huan Pei[†], Li Wang[†,*], Ming-Hua Zeng[‡]

[†]*College of Chemistry and Chemical Engineering, Xinjiang Normal University, Urumqi 830054, China*

[‡] *Key Laboratory for the Synthesis and Application of Organic Functional Molecules, College of Chemistry and Chemical Engineering, Hubei University, Wuhan, 430062 (P. R. China)*

Corresponding Author

* E-mail: wangliresearch@163.com (L. Wang);

Table S1. Crystal data and structure refinement for **1**.

	1
Empirical formula	$In_{14}Se_{33}Sn_2Zn_4C_{16}H_{56}N_8O_8$
Formula weight	5200.71
Temperature (K)	190(2)
Crystal system	tetragonal
space group	$I4_1/acd$
a/ Å	24.3462(2)
b/ Å	24.3462(2)
c/ Å	45.0062(9)
α (deg)	90
β (deg)	90
γ (deg)	90
V (Å^3)	26676.9(7)
Z	8
D (g cm^{-3})	2.590
μ (mm^{-1})	33.112
F (000)	18400.0
Crystal size (mm^3)	0.094 × 0.051 × 0.037
Reflections collected	54817
Independent reflections	4823 [R_{int} = 0.1111, R_{sigma} = 0.0528]
Data/restraints/parameters	4823/0/121
GOF on F^2	1.078
R_1, wR_2 [$F_o^2 > 2\sigma(F_o^2)$][a]	0.0466, 0.1334
R_1, wR_2 (all data)[a]	0.0714, 0.1445

[a] $R_1 = \Sigma||F_o|-|F_c||/\Sigma|F_o|$, and $wR_2 = [\Sigma w(F_o^2 - F_c^2)^2/\Sigma wF_o^4]^{1/2}$ for $F_o^2 > 2\sigma(F_o^2)$.

Table S2. The final coordinates ($\times 10^4$) and equivalent isotropic displacement parameters ($Å^2 \times 10^3$) of non-hydrogen atoms for **1**. U_{eq} is defined as one-third of the trace of the orthogonalized U_{ij} tensor.

Atom	*x*	*y*	*z*	U_{eq}
In/Sn(1)	6812.8(3)	2082.3(3)	939.8(2)	37.9(3)
In/Sn(2)	5731.5(3)	792.9(3)	934.8(2)	37.3(2)
In/Sn(3)	6888.6(3)	943.3(3)	307.5(2)	42.6(3)
In/Sn(4)	5627.3(3)	1977.4(3)	294.5(2)	38.0(3)
Zn(1)	5523.9(6)	3130.9(6)	937.5(3)	34.0(4)
Se(1)	7500	306.6(7)	0	52.8(6)
Se(2)	6384.7(6)	227.8(5)	614.7(3)	52.0(4)
Se(3)	6280.8(6)	1466.1(5)	-51.4(3)	53.4(4)
Se(4)	7499.8(5)	1571.2(6)	614.4(3)	52.3(4)
Se(5)	5035.4(5)	1303.7(5)	602.0(2)	35.5(3)
Se(6)	6294.6(5)	1413.7(5)	1287.4(3)	36.5(3)
Se(7)	6183.3(5)	2676.3(5)	606.9(2)	36.6(3)
Se(8)	5000	2500	-57.0(4)	48.1(5)
Se(9)	7410.6(5)	2711.5(5)	1255.6(3)	48.5(4)
Se(10)	5000	2500	1250	30.7(6)

Table S3. Selected Bond Distances (Å) for **1**

Atom	bond distance	Atom	bond distance
In/Sn(1)-Se(7)	2.5856(14)	In/Sn(3)-Se(3)	2.5337(15)
In/Sn(1)-Se(9)	2.5464(14)	In/Sn(3)-Se(4)	2.5415(15)
In/Sn(1)-Se(6)	2.5859(14)	In/Sn(4)-Se(7)	2.5893(14)
In/Sn(1)-Se(4)	2.5477(14)	In/Sn(4)-Se(5)	2.5852(13)
In/Sn(2)-Se(5)	2.5812(14)	In/Sn(4)-Se(8)	2.5401(12)
In/Sn(2)-Se(9)$^{(a)}$	2.5452(14)	In/Sn(4)-Se(3)	2.5503(14)
In/Sn(2)-Se(6)	2.5849(14)	Zn(1)$^{(a)}$-Se(10)	2.4420(13)
In/Sn(2)-Se(2)	2.5489(14)	Zn(1)-Se(7)	2.4529(17)
In/Sn(3)-Se(2)	2.5399(14)	Zn(1)$^{(b)}$-Se(6)	2.4534(17)
In/Sn(3)-Se(1)	2.5561(12)	Zn(1)$^{(c)}$-Se(5)	2.4553(17)

Symmetry transformations used to generate equivalent atoms:

(a) 1/4+Y, 3/4-X, 1/4-Z; (b) 3/4-Y, -1/4+X; (c) 1-X, 1/2-Y, +Z.

Table S4. Selected Bond Angles (deg) for **1**

Atom	bond angle	Atom	bond angle
Se(7)-In/Sn(1)-Se(6)	114.42(5)	Se(3)-In/Sn(4)-Se(5)	111.40(5)
Se(9)-In/Sn(1)-Se(7)	109.01(5)	Zn(1)$^{(a)}$-Se(10)-Zn(1)$^{(b)}$	109.68(6)
Se(9)-In/Sn(1)-Se(6)	108.66(5)	Zn(1)$^{(c)}$-Se(10)-Zn(1)$^{(a)}$	109.37(3)
Se(9)-In/Sn(1)-Se(4)	103.85(5)	Zn(1)-Se(7)-In/Sn(1)	106.78(5)
Se(4)-In/Sn(1)-Se(7)	109.22(5)	Zn(1)-Se(7)-In/Sn(4)	106.49(6)
Se(4)-In/Sn(1)-Se(6)	111.14(5)	Se(10)-Zn(1)-Se(7)	114.04(6)
Se(5)-In/Sn(2)-Se(6)	115.00(4)	Se(10)-Zn(1)-Se(5)$^{(c)}$	114.65(6)
Se(9)$^{(a)}$-In/Sn(2)-Se(5)	108.38(5)	Se(10)-Zn(1)-Se(6)	114.53(6)
Se(9)$^{(a)}$-In/Sn(2)-Se(6)	108.74(5)	Se(7)-Zn(1)-Se(5)$^{(c)}$	104.06(6)
Se(9)$^{(a)}$-In/Sn(2)-Se(2)	104.87(5)	Se(6)$^{(b)}$-Zn(1)-Se(7)	103.78(6)
Se(2)-In/Sn(2)-Se(5)	109.98(5)	Se(6)$^{(b)}$-Zn(1)-Se(5)$^{(c)}$	104.51(6)
Se(2)-In/Sn(2)-Se(6)	109.37(5)	In/Sn(2)-Se(5)-In/Sn(4)	104.50(5)
Se(2)-In/Sn(3)-Se(1)	99.21(5)	Zn(1)$^{(c)}$-Se(5)-In/Sn(4)	106.42(5)
Se(2)-In/Sn(3)-Se(4)	113.55(5)	Zn(1)$^{(c)}$-Se(5)-In/Sn(2)	106.11(5)
Se(3)-In/Sn(3)-Se(2)	114.17(5)	In/Sn(2)$^{(b)}$-Se(9)-In/Sn(1)	102.72(5)
Se(3)-In/Sn(3)-Se(1)	107.43(4)	In/Sn(2)-Se(6)-In/Sn(1)	104.81(5)
Se(3)-In/Sn(3)-Se(4)	112.72(5)	Zn(1)$^{(a)}$-Se(6)-In/Sn(1)	105.98(5)
Se(4)-In/Sn(3)-Se(1)	108.55(4)	Zn(1)$^{(a)}$-Se(6)-In/Sn(2)	106.67(5)
Se(5)-In/Sn(4)-Se(7)	114.68(4)	In/Sn(4)$^{(c)}$-Se(8)-In/Sn(4)	102.98(6)
Se(8)-In/Sn(4)-Se(7)	108.86(4)	In/Sn(3)-Se(2)-In/Sn(3)	103.82(5)
Se(8)-In/Sn(4)-Se(5)	108.43(4)	In/Sn(3)$^{(d)}$-Se(1)-In/Sn(3)	105.33(7)
Se(8)-In/Sn(4)-Se(3)	103.86(5)	In/Sn(3)-Se(3)-In/Sn(4)	102.74(5)
Se(3)-In/Sn(4)-Se(7)	109.03(5)	In/Sn(3)-Se(4)-In/Sn(1)	102.82(5)

Symmetry codes: (a) 1/4+Y, 3/4-X, 1/4-Z; (b) 3/4-Y, -1/4+X, 1/4-Z; (c) 1-X, 1/2-Y, +Z; (d)

3/2-X,+Y,-Z.

Table S5. The In:Sn ratio determined by inductively coupled plasma-mass spectroscopy (ICP-MS) (5 times)

The percentage of In (%)	The percentage of Sn (%)	Molar ratio of In/Sn
29.76	4.62	6.66
29.74	4.66	6.60
32.04	4.58	7.23
33.48	4.71	7.35
31.82	4.72	6.97

We weighed different amount of **1**, dissolved them into aqua regia, diluted the solution into ppb level (ppb = 1 μg/L), then measured using ICP-MS. Based on the above analyses, we conclude that In:Sn molar ratio is 7:1.

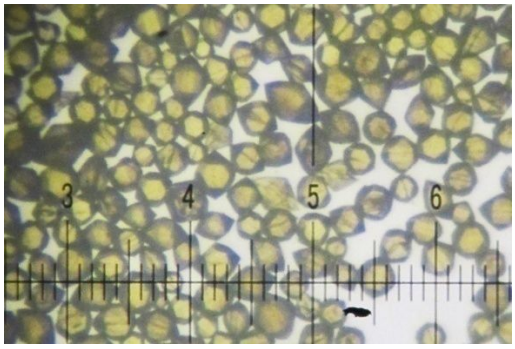

Figure S1. Images for single crystals of compound **1**.

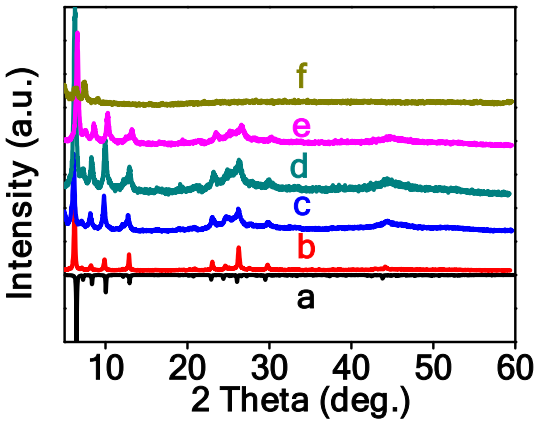

Figure S2. PXRD patterns of (a) calculated (b) Pristine **1** (c) after 1 cycle degradation of MB (d) after 2 cycle degradation of MB (e) after 3 cycle degradation of MB (f) after 400 °C calcination of compound **1**.

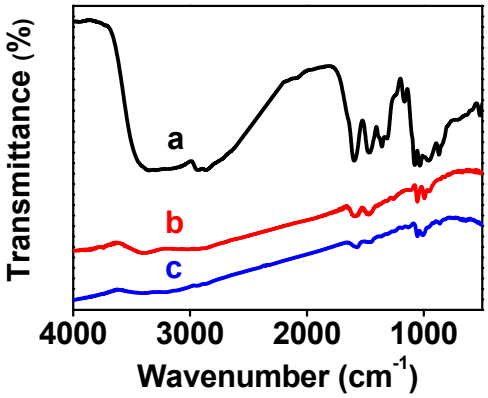

Figure S3. IR spectra of (a) ethanolamine (b) pristine **1** (c) products **1** after degradation 3 cycles of MB.

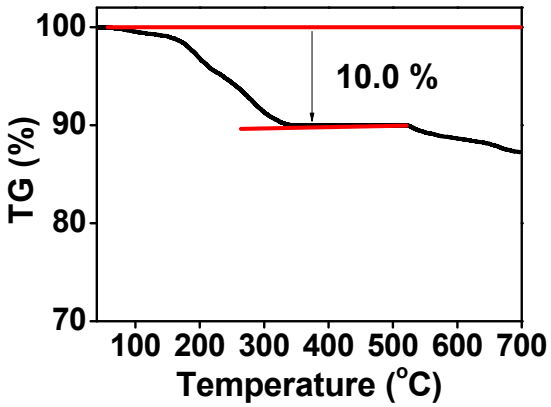

Figure S4.TG curve of **1**.

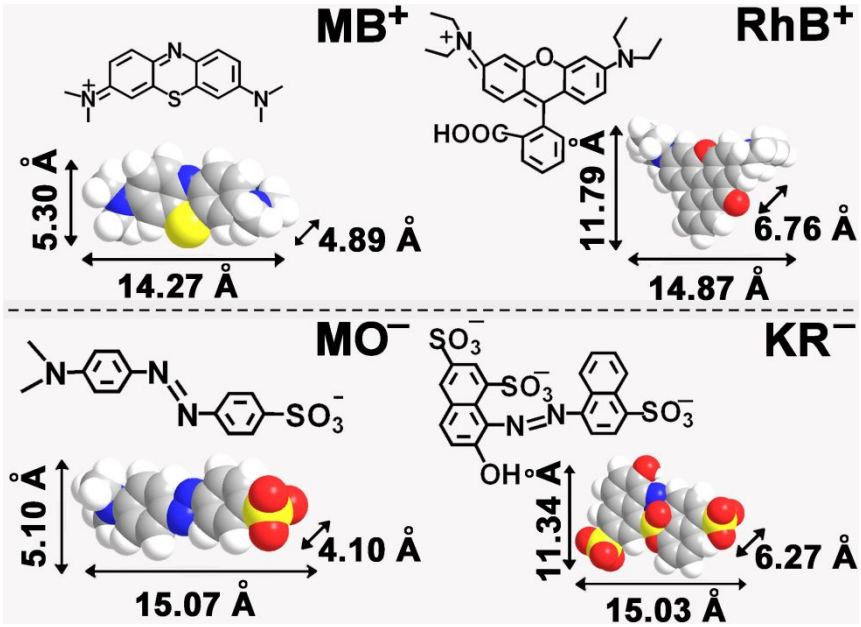

Figure S5. Chemical structures and dimensions (Å) of different dye molecules.

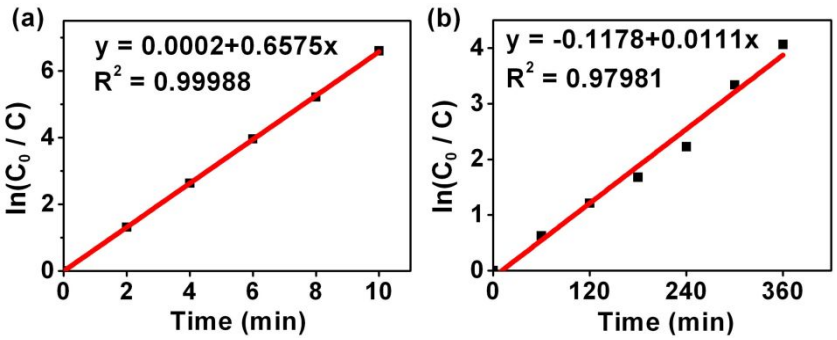

Figure S6. Linear plots of $\ln(C_0/C)$ for the photocatalytic degradation of (a) MB and (b) RhB respectively.

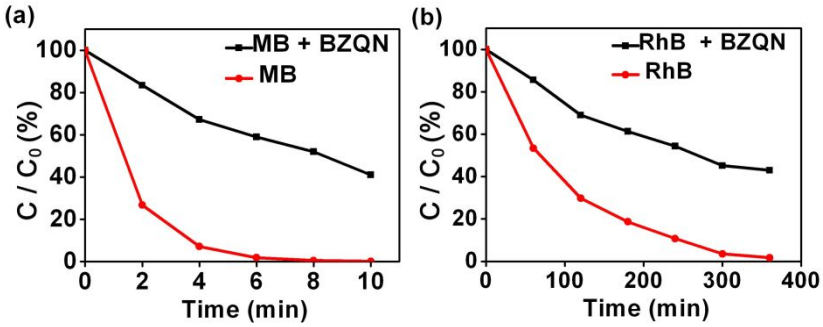

Figure S7. Control experiments using scavenger (benzoquinone, BZQN) of superoxide radicals for the photocatalytic degradation of MB (a) and RhB (b) under visible light irradiation conditions.

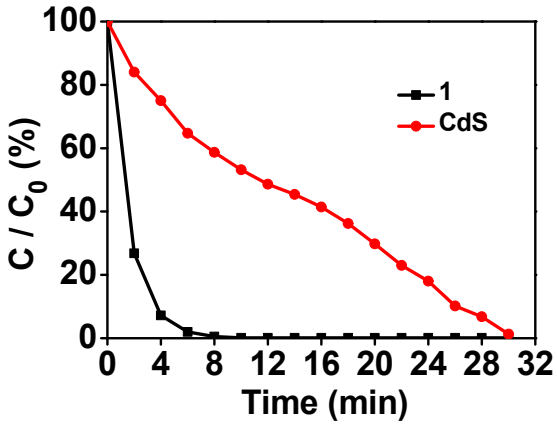

Figure S8. Photocatalytic activities of CdS, Zeolite and **1** for MB decomposition under visible light irradiation conditions.

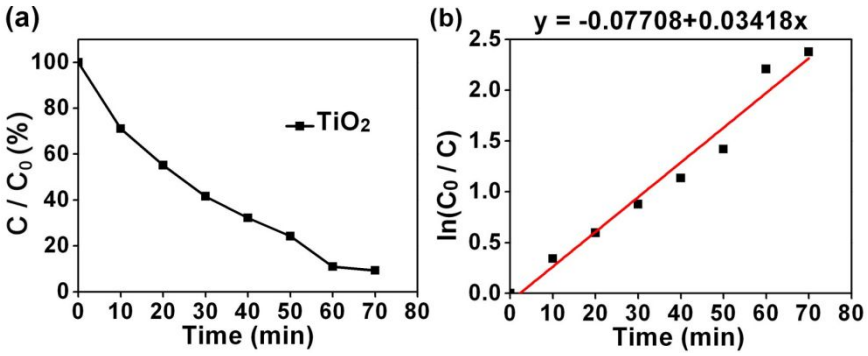

Figure S9. (a) Photocatalytic degradation curve of MB in the presence of TiO_2. (b) Linear plots of $\ln(C_0/C)$ for the photocatalytic degradation of MB.